Supporting Information for

Atomistic Origins of Co-doping-induced Type Conversion in Nitrogen-doped

Graphene

Hyo Seok Kim, Han Seul Kim, Seong Sik Kim, and Yong-Hoon Kim*

Graduate School of EEWS, KAIST, 291 Daehak-ro, Yuseong-gu, Daejeon 305-701, Korea
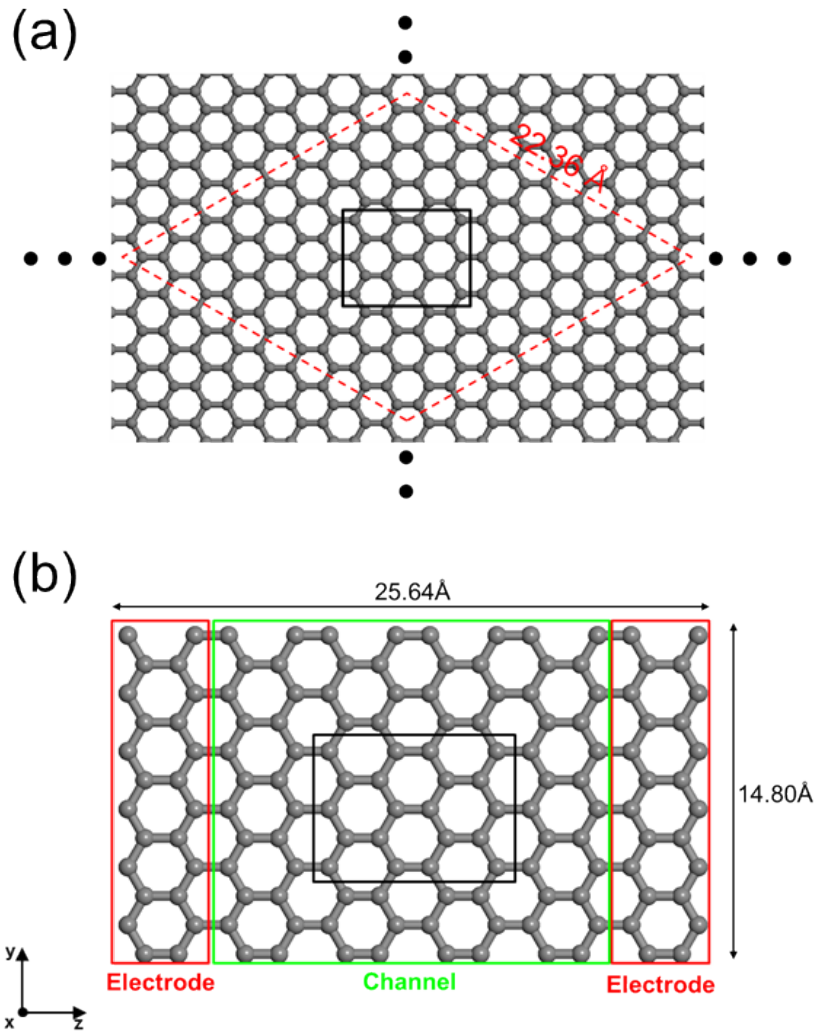
E-mail: y.h.kim@kaist.ac.kr

Figure S1. (a) Graphene models employed in the density functional theory (DFT) calculations of the N-doped graphenes (NGs). The red dashed box is the 9×9 unit cell of graphene used to generate the pyridinic NG with monovacancy (V_1-N^{py}), pyridinic NG with divacancy (V_2-N^{py}), nitrilic NG (N^{nit}), and pyrrolic NG (N^{pyrr}) models. (b) Atomic models for the non-equilibrium Green's function (NEGF) calculations. The system is composed of four unit cells for the channel region and one unit cell for the semi-infinite electrodes. Along the transverse direction, six unit cells were adopted. Black boxes in (a) and (b) represent the regions used to show the atomic structures in Figures 1, 4, and 5.
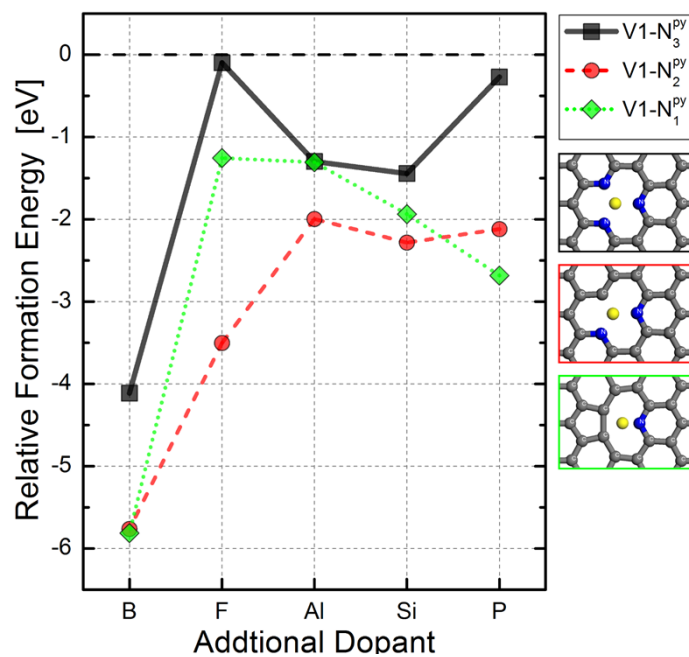
Figure S2. Relative formation energies of introducing an additional dopant atom into V_1-N^{py}_3 (black squares), V_1-N^{py}_2 (red circles), and V_1-N^{py}_1 (green diamonds).
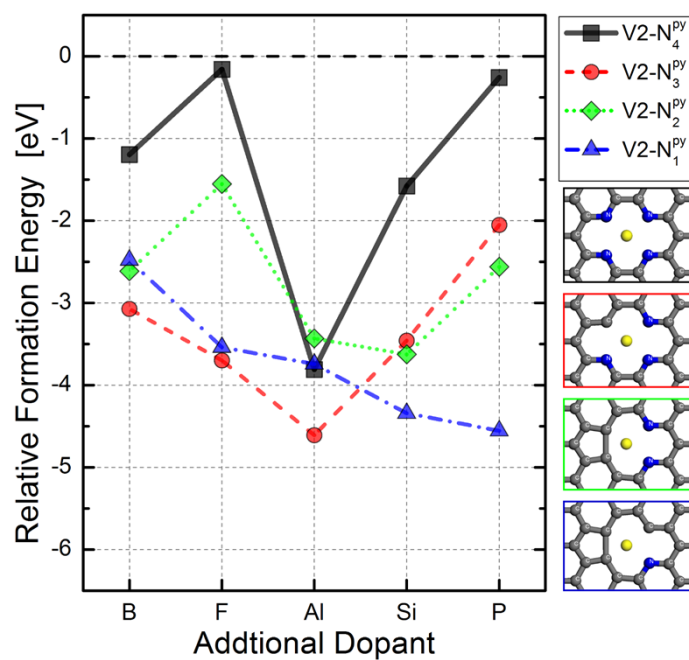

Figure S3. Relative formation energies of introducing an additional dopant atom into V_1-N^{py}_4 (black squares), V_1-N^{py}_3 (red circles), V_1-N^{py}_2 (green diamonds), and V_1-N^{py}_2 (blue triangles).
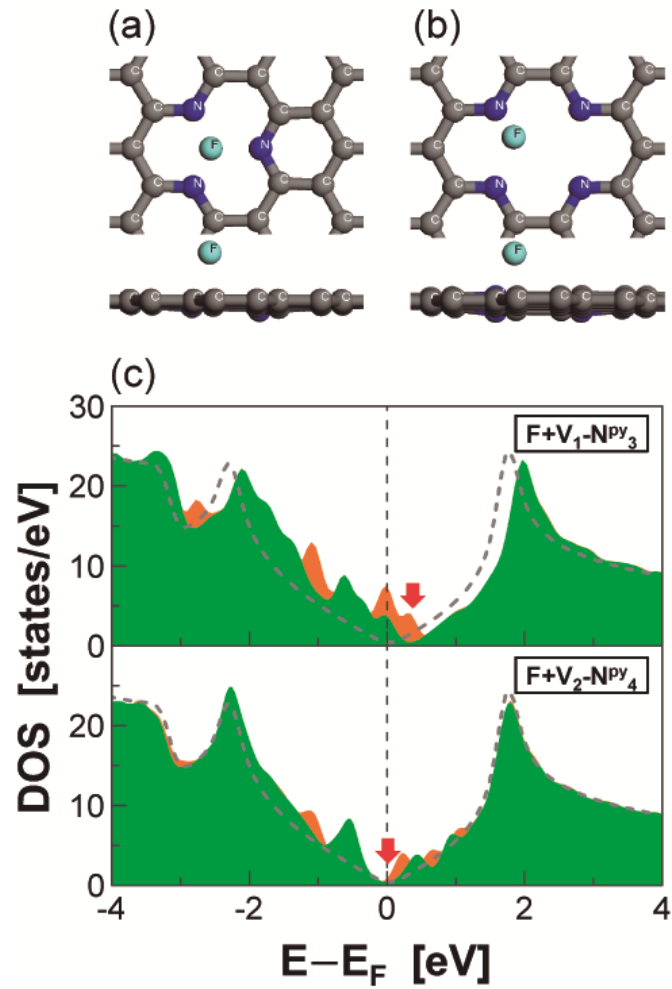
Figure S4. Atomic structures of (a) $F+V_1\text{-}N^{py}_3$, and (b) $F+V_1\text{-}N^{py}_4$. (c) DOS of $F+V_1\text{-}N^{py}_3$ and $F+V_2\text{-}N^{py}_4$. In the DOS plots, pristine graphene DOS are shown together (gray dashed lines), and the Dirac points are marked by red arrows. We show both the majority (green filled lines) and minority (orange filled lines) DOS.
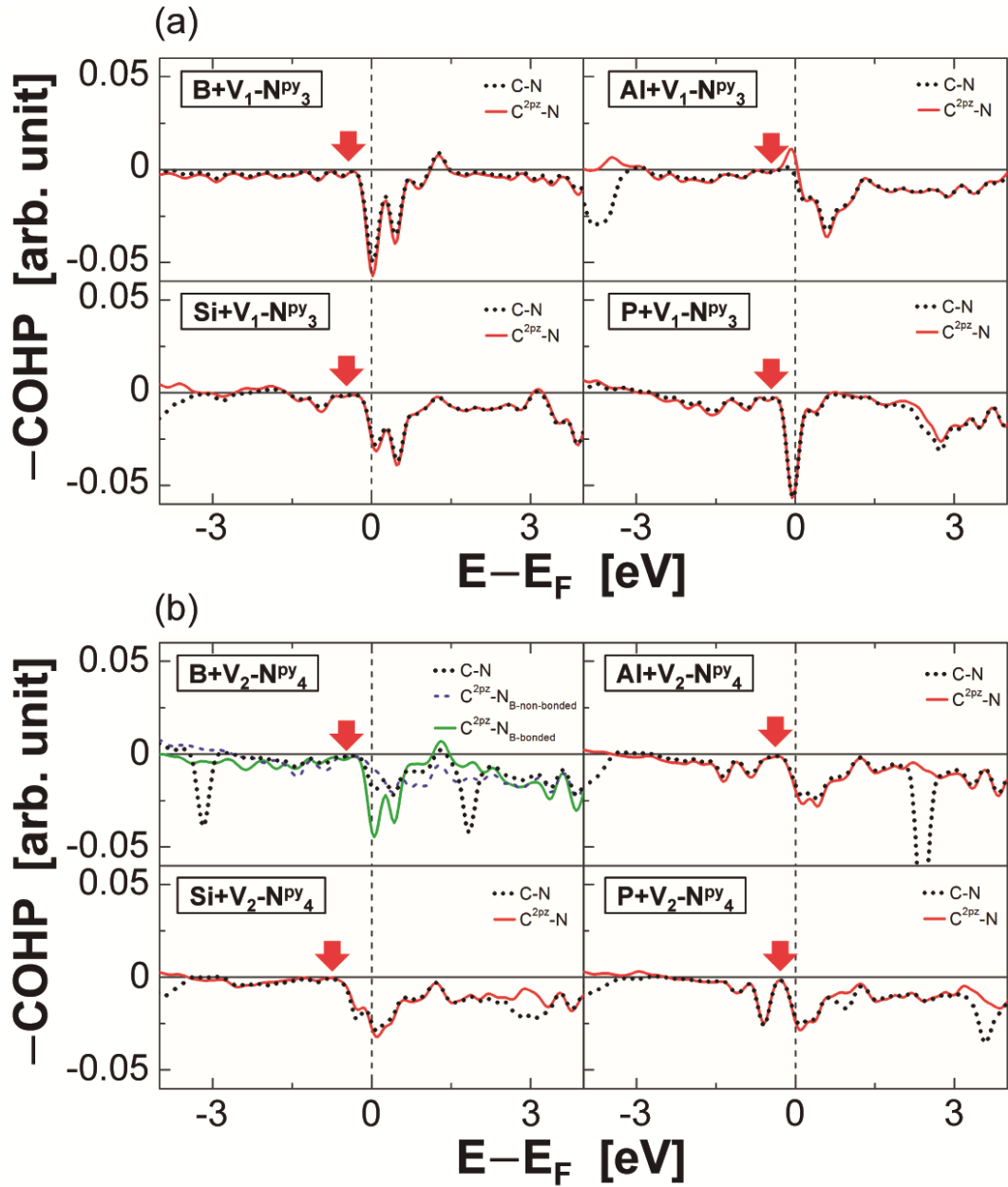
Figure S5. Decompositions of the total C-N COHPs (dotted lines, reproduced from Fig. 4) for (a) $X+V_1$-N^{py}_3 and (b) $X+V_2$-N^{py}_4. The C $2p_z$-N COHP (red solid line) is shown for $X+V_1$-N^{py}_3 and $X+V_2$-N^{py}_4. For B+V_2-N^{py}_4, the C $2p_z$-N COHPs have been decomposed into the one for the two N atoms bonded with B ($N_{B\text{-bonded}}$, green solid line) and the other two N atoms not bonded with B ($N_{B\text{-non-bonded}}$, blue dashed line). Note that, while a strong antibonding peak above E_D for C $2p_z$-$N_{B\text{-bonded}}$, it is absent for $2p_z$-$N_{B\text{-bonded}}$ COHP component.
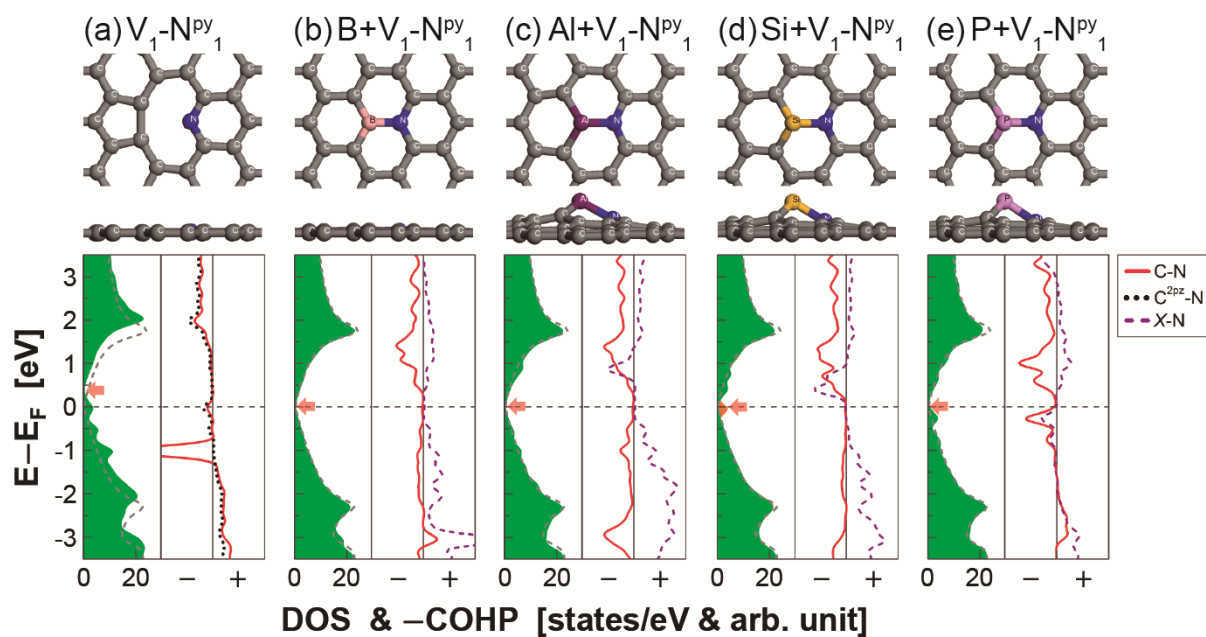
Figure S6. Atomic structures (top panels), DOS (bottom left panels), and COHPs (bottom right panels) of (a) V_1-N^{py}_1, (b) B+V_1-N^{py}_1, (c) Al+V_1-N^{py}_1, (d) Si+V_1-N^{py}_1, and (e) P+V_1-N^{py}_1. In the DOS plots, pristine graphene DOS are shown together (gray dashed lines), and the Dirac points are marked by red arrows. In the COHP plots, the C-N (red solid lines), C $2p_z$-N (black dotted line in the bottom right panel of Figure S6a), and X-C (purple dashed lines) COHPs are shown. For the slightly spin-polarized Si+V_1-N^{py}_1 case, we show both the majority (green filled lines) and minority (orange filled lines) DOS.
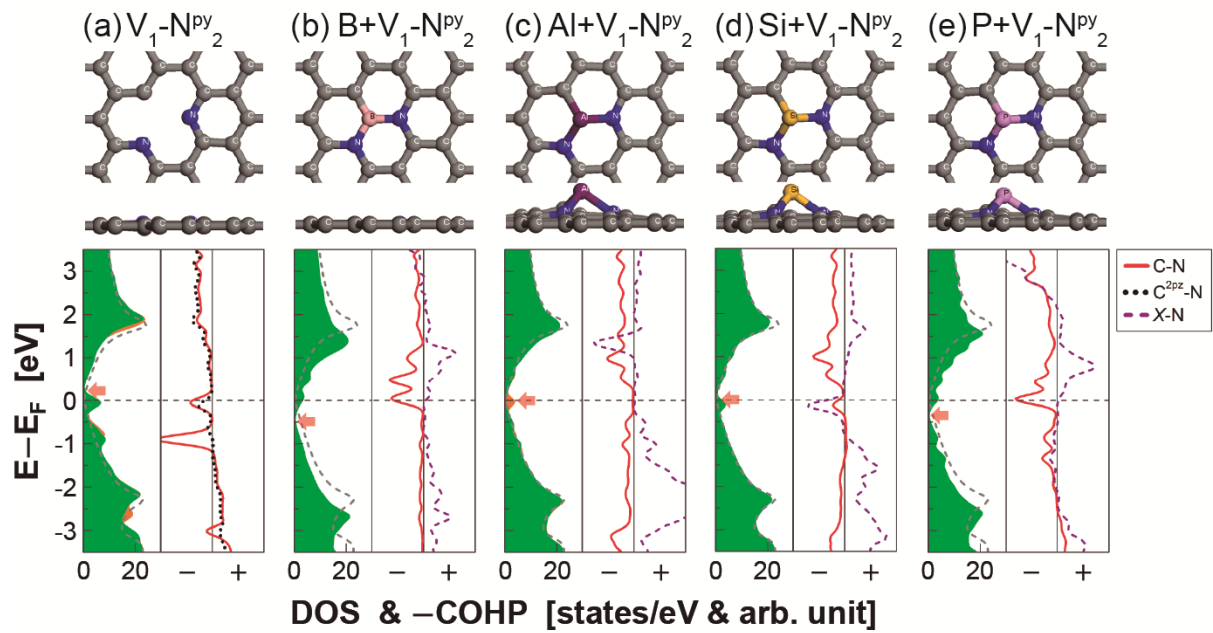
Figure S7. Atomic structures (top panels), DOS (bottom left panels), and COHPs (bottom right panels) of (a) V_1-N^{py}_2, (b) B+V_1-N^{py}_2, (c) Al+V_1-N^{py}_2, (d) Si+V_1-N^{py}_2, and (e) P+V_1-N^{py}_2. In the DOS plots, pristine graphene DOS are shown together (gray dashed lines), and the Dirac points are marked by red arrows. In the COHP plots, the C-N (red solid lines), C $2p_z$-N (black dotted line in the bottom right panel of Figure S7a), and X-C (purple dashed lines) COHPs are shown. For the slightly spin-polarized V_1-N^{py}_2 and Al+V_1-N^{py}_2 cases, we show both the majority (green filled lines) and minority (orange filled lines) DOS.
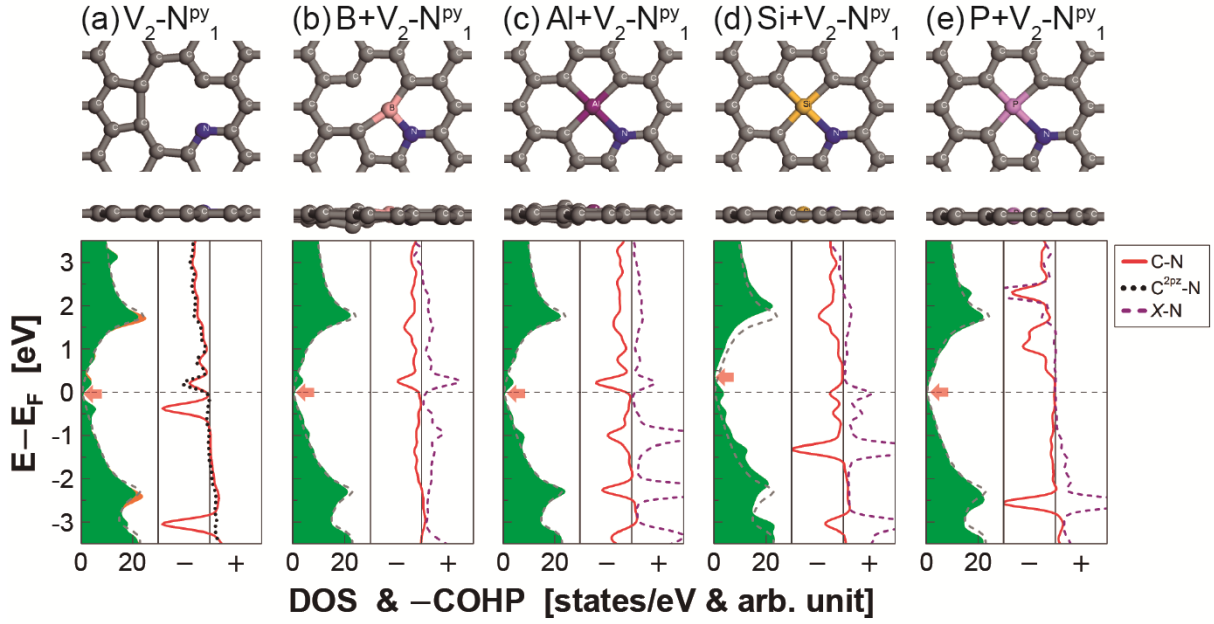
Figure S8. Atomic structures (top panels), DOS (bottom left panels), and COHPs (bottom right panels) of (a) V_2-N^{py}_1, (b) B+V_2-N^{py}_1, (c) Al+V_2-N^{py}_1, (d) Si+V_2-N^{py}_1, and (e) P+V_2-N^{py}_1. In the DOS plots, pristine graphene DOS are shown together (gray dashed lines), and the Dirac points are marked by red arrows. In the COHP plots, the C-N (red solid lines), C $2p_z$-N (black dotted line in the bottom right panel of Figure S8a), and X-C (purple dashed lines) COHPs are shown. For the slightly spin-polarized V_2-N^{py}_1 case, we show both the majority (green filled lines) and minority (orange filled lines) DOS. The Si+V_2-N^{py}_1 case is one of the two exceptions (out of the 28 total V-N^{py} cases analyzed in Figure 4 and Figures S6—S10) in which the p-type character survives even after the introduction of a codoping B/Al/Si/P atom (The other case is B+V_2-N^{py}_2. See Figure S9b and the corresponding discussion). Although the Si atom is fourfold coordinated with the surrounding three C and one N atoms, the C-N antibonding COHP peak still remains below E_D and is pinned at E_F. In the P+V_2-N^{py}_1 case, the antibonding COHP peak disappears and the bipolar type is obtained.
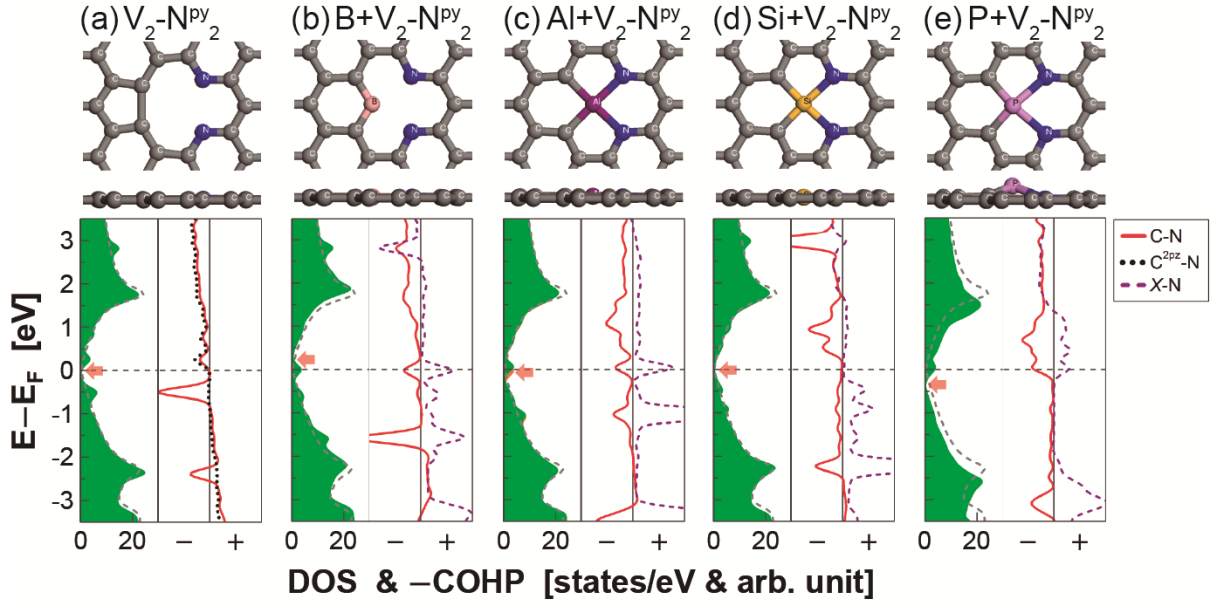
Figure S9. Atomic structures (top panels), DOS (bottom left panels), and COHPs (bottom right panels) of (a) V_2-N^{py}_2, (b) $B+V_2$-N^{py}_2, (c) $Al+V_2$-N^{py}_2, (d) $Si+V_2$-N^{py}_2, and (e) $P+V_2$-N^{py}_2. In the DOS plots, pristine graphene DOS are shown together (gray dashed lines), and the Dirac points are marked by red arrows. In the COHP plots, the C-N (red solid lines), C $2p_z$-N (black dotted line in the bottom right panel of Figure S9a), and X-C (purple dashed lines) COHPs are shown. For the slightly spin-polarized $Al+V_2$-N^{py}_2 case, we show both the majority (green filled lines) and minority (orange filled lines) DOS. The $B+V_2$-N^{py}_2 case is another exception where the p-type character survives even after the introduction of a codoping B/Al/Si/P atom (The other case is $Si+V_2$-N^{py}_1. See Figure S8d and the corresponding discussion). As in the cases of $F+V_1$-N^{py}_3 and $F+V_1$-N^{py}_4 (Figure S6), this results from the inability of the codoping B atom to establish bonding with the two surrounding N atoms. This again emphasizes that the precondition of the applicability of our codoping approach is the structural annealing of the vacancy defects.
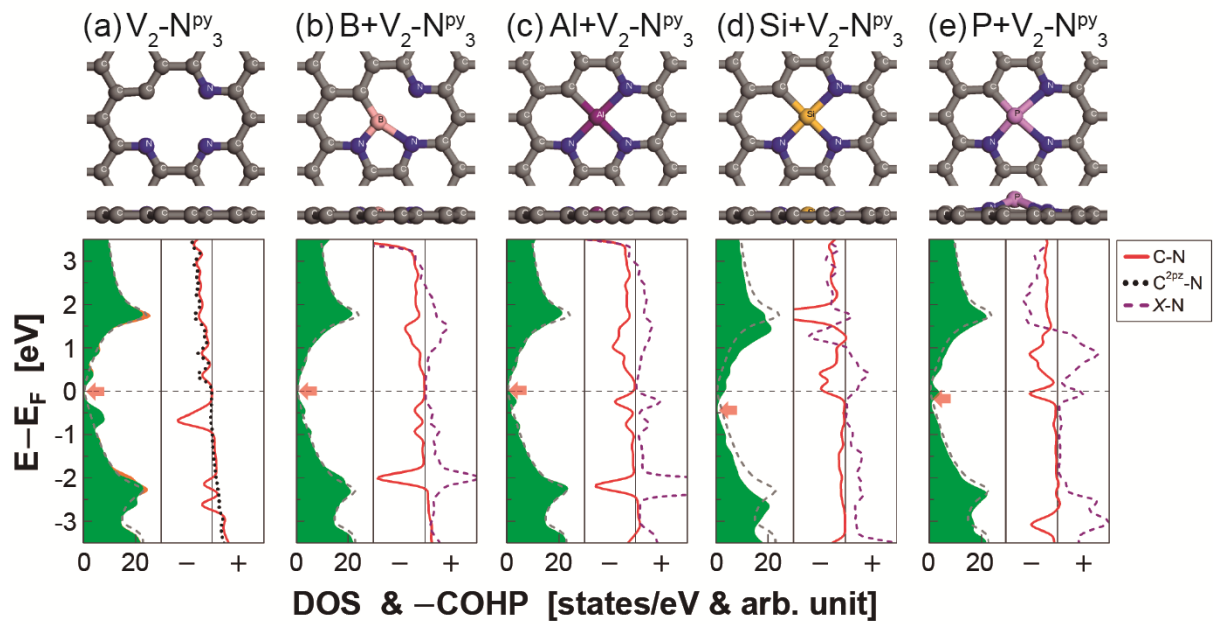
Figure S10. Atomic structures (top panels), DOS (bottom left panels), and COHPs (bottom right panels) of (a) V_2-N^{py}_3, (b) B+V_2-N^{py}_3, (c) Al+V_2-N^{py}_3, (d) Si+V_2-N^{py}_3, and (e) P+V_2-N^{py}_3. In the DOS plots, pristine graphene DOS are shown together (gray dashed lines), and the Dirac points are marked by red arrows. In the COHP plots, the C-N (red solid lines), C $2p_z$ -N (black dotted line), and X-C (purple dashed lines) COHPs are shown. For the slightly spin-polarized V_2-N^{py}_3 case, we show both the majority (green filled lines) and minority (orange filled lines) DOS.
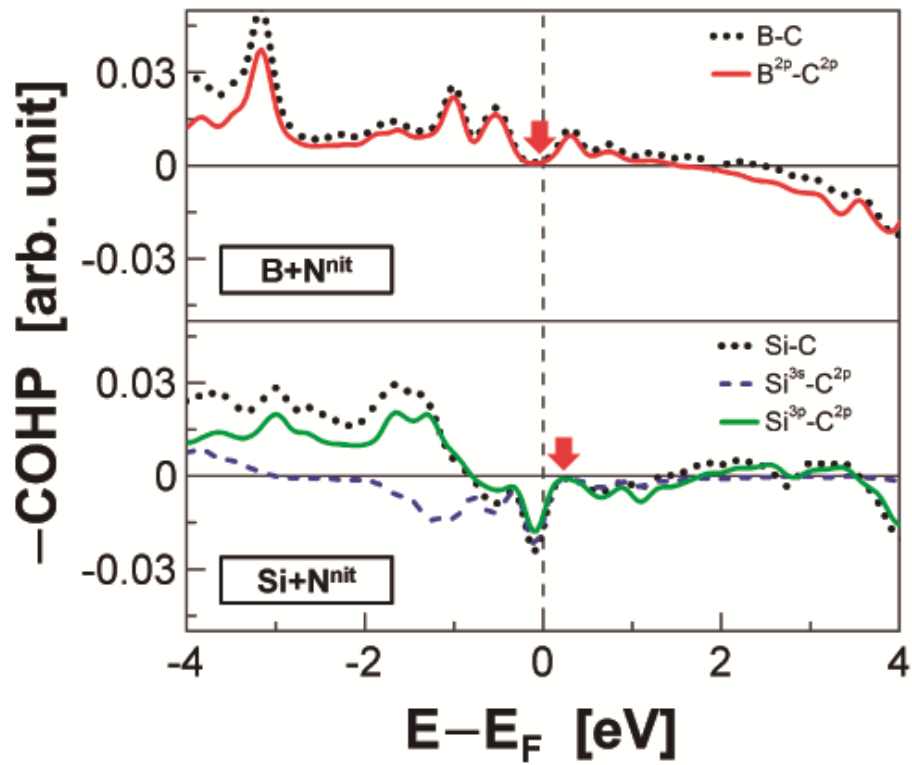
Figure S11. Decompositions of the total *X*-C COHPs [dotted lines, reproduced from Fig. 4] for B+N^{nit} and Si+N^{nit}. The B 2p -C 2p COHP (red solid line) is shown for B+N^{nit}. For Si+N^{nit}, the Si 3p -C 2p COHP (green solid line) and Si 3s -C 2p COHP (blue dashed line) are shown.